[Chem. Pharm. Bull. 34(6)2330—2340(1986)]

Electron Paramagnetic Resonance Studies of Hydrogen Bonding in Low-Spin Ferric Heme Complexes. Methoxo(*N*-methylimidazole)tetraphenylporphinatoiron(III) in Dimethyl Sulfoxide–Methanol and Related Systems

TOMOKO OTSUKA, TOSHIE OHYA, and MITSUO SATO*

Faculty of Pharmaceutical Sciences, Teikyo University, Sagamiko, Kanagawa 199–01, Japan

(Received October 25, 1985)

Electron paramagnetic resonance (EPR) spectroscopy has been employed to characterize the hydrogen-(H-) bonded state of the mixed-ligand low-spin complex Fe(TPP) (OMe) (NMeIm), which is formed upon mixing of Fe(TPP) (OMe) with NMeIm in Me_2SO–MeOH. Two spectrally distinct low-spin species, designated A and B in increasing order of g anisotropy, were detected depending upon the MeOH concentration in the solvent. The two low-spin species differ in degree of H-bond formation between the coordinated MeO^- and the solvent MeOH. The H-bond formation proceeds in one step, by EPR criteria, A and B being regarded as in the initial and final H-bonded states, respectively. The H-bonding interaction results in a decreased crystal field around the iron, thereby causing the tetragonal and rhombic splittings in the t_2 orbitals to decrease on going from A to B.

Keywords——electron paramagnetic resonance; low-spin ferric heme complex; hydrogen bonding; methoxo(*N*-methylimidazole) tetraphenylporphinatoiron(III); crystal field splitting

Introduction

Hydrogen-(H-) bonding interaction in which the axial ligands of iron porphyrin (heme) complexes take part has attracted much interest in recent years because of its crucial role in modulating the electronic and reactive properties at the central metal ion.[1-3] EPR[4] spectroscopy characterizes the electronic structural changes in Fe(III) states which are caused by the H bonding. For example, it has been demonstrated for model low-spin complexes Fe(PPIX) $(ImH)_2^+$,[5,6] Fe(PPIXDME) $(ImH)_2^+$,[6] and Fe(TPP) $(ImH)_2^+$[4,7,8] that H bonding or deprotonation of the N–H moiety of coordinated ImH leads to an increased crystal field around the iron, thereby causing alterations in *d*-orbital energy levels. In contrast, we have recently shown that the crystal field in the model low-spin complex Fe(TPP) $(OMe)_2^-$ decreases with increasing H-bonding interaction between the coordinated MeO^- and solvent MeOH.[9] The opposite trends in the crystal field alterations between the two model systems are reasonably explained by the fact that the axial ligand acts as an H-bond donor in, *e.g.*, Fe(TPP) $(ImH)_2^+$, while it acts as an H-bond acceptor in Fe(TPP) $(OMe)_2^-$.

In the present paper, we report on the H-bonding interaction found in the mixed-ligand low-spin complex Fe(TPP) (OMe) (NMeIm) that is formed upon mixing of Fe(TPP) (OMe) with NMeIm in Me_2SO–MeOH. The H-bond formation process in Fe(TPP) (OMe) (NMeIm) is expected to be much simpler than in Fe(TPP) $(OMe)_2^-$, since the coordinated NMeIm cannot take part in H-bond formation. In fact, the mixed-ligand complex Fe(TPP) (OMe) (NMeIm) is found to exist in two spectrally distinct states with different sets of g values, as contrasted with the three distinct states of Fe(TPP) $(OMe)_2^-$.[9] It is shown that the H-bond formation between the coordinated MeO^- and the solvent MeOH leads to a decreased crystal

field and electron density at the iron. Such electronic alterations in Fe(TPP) (OMe) (NMeIm) are compared with those in Fe(TPP) $(OMe)_2^-$ [9] and Fe(TPP) $(ImH)_2^+$ [7,8] and are discussed in connection with the crystal field parameters obtained from the observed g values. Similar results have been obtained with the mixed-ligand complex Fe(TPP) (OMe) (py), details of which will also be reported in the present paper.

Experimental

Materials——Fe(TPP) (OMe) was prepared as described previously[10] using chlorin-free $TPPH_2$[11] as the starting material. NMeIm was purified by distillation from BaO, while py, lut, and coll were distilled from CaH_2, and phen was sublimed prior to use. Me_2SO and toluene were purified as described previously[9,10] and were stored over 4A molecular sieves. CH_2Cl_2 was distilled from P_2O_5 immediately prior to use. MeOH was of spectrograde quality (Dojin Chemicals) and was used without further purification.

Procedures——EPR samples were prepared by adding NMeIm or py to 0.3—1.5 mM solutions of Fe(TPP) (OMe) in Me_2SO–MeOH, CH_2Cl_2–MeOH, and toluene–MeOH with vigorous shaking at room temperature. The initial concentration ratio $[NMeIm]_0/[Fe(TPP)(OMe)]_0$ or $[py]_0/[Fe(TPP)(OMe)]_0$ was varied systematically in the range of 1—1500, and the MeOH concentration in the mixed solvents, in the range of 1—25% (v/v). For some experiments, a known weight of lut, coll, or phen was further added to give concentrations of 100—700 mM. The sample solutions were transferred into quartz tubes (4.0 mm i.d.) and were frozen at 77 K within a few minutes to avoid side reactions.

Measurements——EPR measurements were made at 77 K or below with a JEOL FE3AX spectrometer with 100-kHz field modulation. The magnetic field was calibrated with an NMR gaussmeter (ES-FC4, JEOL), and the microwave frequency was determined by use of a DPPH reference ($g=2.0036$). The g values were determined at the peak (or trough) and at the middle point of the first derivative spectrum. Temperatures below 77 K were attained with a Heli-tran variable-temperature system (LTD-3-110, Air Products Co.). Visible spectra were recorded on a Hitachi 200-10 spectrophotometer with 2—10 mm quartz cells at room temperature.

Results and Discussion

Formation of Fe(TPP) (OMe) (NMeIm) and Fe(TPP) (OMe) (py)

As shown in Fig. 1, addition of NMeIm to Fe(TPP) (OMe) in Me_2SO–MeOH results in the formation of two distinct low-spin species which are both assigned to the mixed-ligand complex Fe(TPP) (OMe) (NMeIm). The two species are interpreted as being different in degree of H-bond formation between the coordinated MeO^- and the solvent MeOH (*vide infra*).

Note that only the nearest axial coordination is represented by the formula Fe(TPP) (OMe) (NMeIm). Thus, the reaction leading to the two low-spin species is written simply as:

$$\text{Fe(TPP) (OMe)} + \text{NMeIm} = \text{Fe(TPP) (OMe) (NMeIm)} \qquad (1)$$

It can be seen from Fig. 1b that addition of *ca.* 2 eq of NMeIm is sufficient for completion of the adduct formation. In contrast to this observation, no visible spectral change was detected at room temperature even with *ca.* 30 eq of NMeIm added. It appears that reaction 1 is highly exothermic and Fe(TPP) (OMe) (NMeIm) is formed and stabilized only at low temperature. In fact, the sample solution changed from moss green to reddish brown upon freezing at 77 K.

With a large excess of NMeIm (100—1500 eq), the bis-ligand complex is formed as a minor product (Figs. 1c and d) according to:

$$\text{Fe(TPP) (OMe) (NMeIm)} + \text{NMeIm} = \text{Fe(TPP) (NMeIm)}_2^+ + \text{MeO}^- \qquad (2)$$

Visible spectra indicated only the partial conversion of Fe(TPP) (OMe) into Fe(TPP) $(NMeIm)_2^+$ and no evidence was obtained for the complex species Fe(TPP) (OMe) (NMeIm) existing in solution at room temperature. Thus, the preferential formation of Fe(TPP) (OMe) (NMeIm) in frozen solutions as demonstrated by EPR absorptions is attributed to a marked temperature dependence of K_1. Probably, $K_1 \ll K_2$ at room temperature and K_1 increases

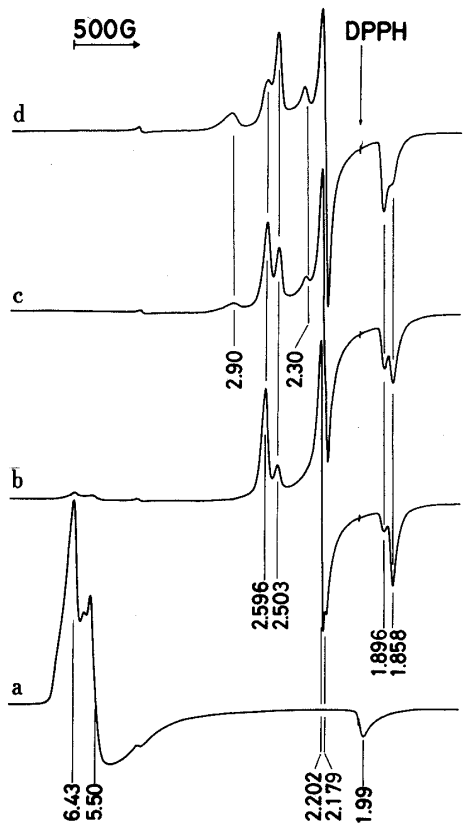

Fig. 1. EPR Spectra at 20 K of Fe(TPP) (OMe) plus NMeIm in Me_2SO–MeOH (90 : 10, v/v)

Conditions: $[Fe(TPP)(OMe)]_0 = 0.70$ mM; $[NMeIm]_0/[Fe(TPP)(OMe)]_0 = 0$ (a), 2.0 (b), 180 (c), and 900 (d). The spectra indicate that there are four complex species in the solutions. They are assigned as Fe(TPP) (OMe) (high spin; $g_x = 5.50$, $g_y = 6.43$, $g_z = 1.99$), Fe(TPP) (OMe) (NMeIm) species A (low spin; $g_x = 1.896$, $g_y = 2.179$, $g_z = 2.503$), Fe(TPP)(OMe) (NMeIm) species B (low spin; $g_x = 1.858$, $g_y = 2.202$, $g_z = 2.596$), and Fe(TPP) $(NMeIm)_2^+$ (low spin; $g_x = 1.57$ (not shown), $g_y = 2.30$, $g_z = 2.90$) with the spin state and g values in parentheses. Peak assignments are indicated on the figure.

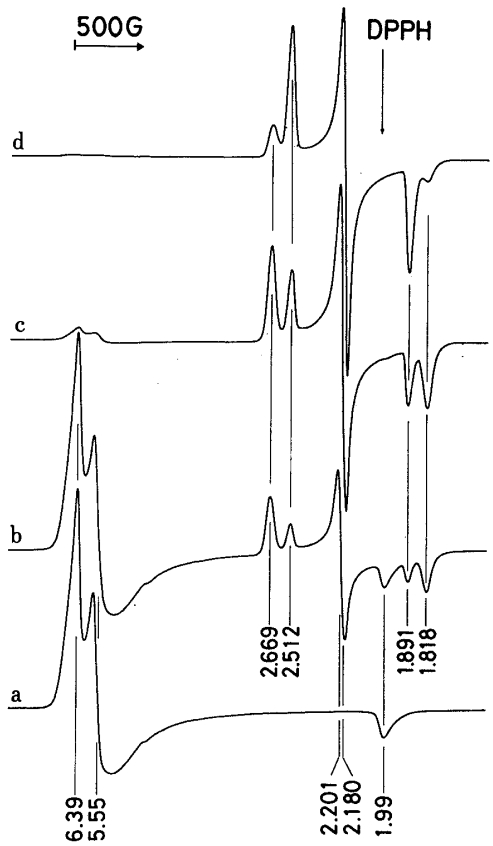

Fig. 2. EPR Spectra at 20 K of Fe(TPP) (OMe) plus py in Toluene–MeOH (75 : 25, v/v)

Conditions: $[Fe(TPP)(OMe)]_0 = 1.40$ mM; $[py]_0/[Fe(TPP)(OMe)]_0 = 0$ (a), 4.5 (b), 90 (c), and 900 (d). The spectra indicate that there are three complex species in the solutions. They are assigned as Fe(TPP) (OMe) (high spin; $g_x = 5.55$, $g_y = 6.39$, $g_z = 1.99$), Fe(TPP) (OMe) (py) species A (low spin; $g_x = 1.891$, $g_y = 2.180$, $g_z = 2.512$), and Fe(TPP) (OMe) (py) species B (low spin; $g_x = 1.818$, $g_y = 2.201$, $g_z = 2.669$) with the spin state and g values in parentheses. Peak assignments are indicated on the figure.

rapidly with decreasing temperature, where K_1 and K_2 are the equilibrium constants of reactions 1 and 2, respectively.

Most important, the low-spin complex Fe(TPP) (OMe) (NMeIm) in Me_2SO–MeOH exhibits two different sets of g values, indicating that the low-spin complex is in two electronically distinct states. Two such distinct low-spin species were detected for Fe(TPP) (OMe) (NMeIm) in CH_2Cl_2–MeOH and toluene–MeOH and also for Fe(TPP) (OMe) (py) in the same solvent systems. In Fig. 2 are shown typical EPR spectra observed upon addition of py to Fe(TPP) (OMe) in toluene–MeOH, the formation of two distinct low-spin species Fe(TPP) (OMe) (py) being well demonstrated. The g values obtained at 77 and 20 K are collected in Table I, and the two distinct low-spin species are designated A and B in increasing order of g anisotropy.

This finding is, however, in contrast to the previous observation that the low-spin complex Fe(OEP) (OMe) (NMeIm) or Fe(PPIXDME) (OEt) (py) exhibits a single set of g values in frozen toluene.[12] Probably, the presence of MeOH in our solvent systems is responsible for this discrepancy. EPR spectra of Fe(TPP) (OMe) (NMeIm) and Fe(TPP)

TABLE I. EPR Data for Hydrogen-Bonded Species of Low-Spin Fe(III) Heme Complexes

Low-spin complex/solvent H-bonded species	Observed g values				Crystal field parameters			
	Temp. (K)	g_x	g_y	g_z	$\delta^{a)}$	$\mu^{a)}$	$R^{b)}$	k
Fe(TPP) (OMe) (NMeIm)/Me_2SO–MeOH								
Species A	77	1.896	2.179	2.504	7.46	4.10	0.550	1.040
	20	1.896	2.179	2.503	7.45	4.10	0.551	1.038
Species B	77	1.860	2.201	2.595	6.61	3.55	0.536	1.072
	20	1.858	2.202	2.596	6.53	3.53	0.540	1.068
Fe(TPP) (OMe) (NMeIm)/CH_2Cl_2–MeOH								
Species A	77	1.890	2.178	2.505	7.20	3.98	0.553	1.015
	20	1.891	2.181	2.509	7.23	4.01	0.555	1.029
Species B	77	1.860	2.201	2.590	6.55	3.55	0.542	1.064
	20	1.860	2.201	2.590	6.55	3.55	0.542	1.064
Fe(TPP) (OMe) (NMeIm)/toluene–MeOH								
Species A	77	1.906	2.173	2.478	7.77	4.31	0.555	1.034
	20	1.906	2.174	2.479	7.76	4.32	0.556	1.037
Species B	77	1.863	2.198	2.580	6.60	3.59	0.543	1.056
	20	1.861	2.200	2.585	6.55	3.56	0.544	1.059
Fe(TPP) (OMe) (py)/Me_2SO–MeOH								
Species A	77	1.883	2.180	2.535	7.25	3.84	0.530	1.038
	20	1.883	2.181	2.536	7.24	3.84	0.531	1.041
Species B	77	1.816	2.196	2.673	6.14	3.03	0.494	1.052
	20	1.813	2.199	2.677	6.05	3.02	0.499	1.053
Fe(TPP) (OMe) (py)/CH_2Cl_2–MeOH								
Species A	77	1.878	2.182	2.544	7.10	3.76	0.530	1.036
	20	1.877	2.186	2.547	7.00	3.76	0.537	1.041
Species B	77	1.815	2.197	2.677	6.13	3.03	0.494	1.056
	20	1.813	2.198	2.679	6.08	3.01	0.495	10.54
Fe(TPP) (OMe) (py)/toluene–MeOH								
Species A	77	1.892	2.177	2.511	7.41	4.01	0.541	1.032
	20	1.891	2.180	2.512	7.30	4.00	0.548	1.033
Species B	77	1.818	2.200	2.663	6.03	3.07	0.508	1.047
	20	1.816	2.201	2.669	6.02	3.05	0.507	1.051
Fe(TPP) $(OMe)_2^-$/Me_2SO–MeOH[c)]								
Species I	15	1.942	2.134	2.394	10.62	5.30	0.499	1.039
Species II	15	1.928	2.151	2.442	9.49	4.82	0.508	1.062
Species III	15	1.914	2.165	2.494	8.85	4.43	0.501	1.096
Fe(TPP) $(ImH)_2^+$/CH_2Cl_2[d)]	77	1.56	2.30	2.92	3.35	2.05	0.612	1.055
Fe(TPP) (Im) (ImH)/CH_2Cl_2[d)]	77	1.74	2.28	2.73	4.20	2.73	0.650	1.051
Fe(TPP) $(Im)_2^-$/CH_2Cl_2[d)]	77	1.76	2.28	2.73	4.47	2.84	0.636	1.083

a) In units of ζ (spin-orbit coupling constant, $\zeta \simeq 400\,cm^{-1}$). *b*) $R=\mu/\delta$. *c*) H-bond formation between the iron-bound MeO^- and solvent MeOH proceeds stepwise as the MeOH concentration increases, and species I—III are assigned to the initial, intermediate, and final H-bonded states, respectively. For details, see reference 9. *d*) Taken from reference 7. Im^- refers to imidazolate anion or strongly H-bonded imidazole.

(OMe) (py) measured in pure solvents have confirmed the above view, only a single low-spin species with rather broader line width and with g values similar to those of species A being observed.

Interconversion of Hydrogen-Bonded States. Fe(TPP) (OMe) (NMeIm) in Me_2SO–MeOH

Among the various systems summarized in Table I, the system Fe(TPP) (OMe) (NMeIm) in Me_2SO–MeOH was studied in most detail for the purpose of comparison with the previously reported system Fe(TPP) $(OMe)_2^-$ in Me_2SO–MeOH.[9)] EPR spectra of species A and B of Fe(TPP) (OMe) (NMeIm) were found to vary in relative intensities depending upon

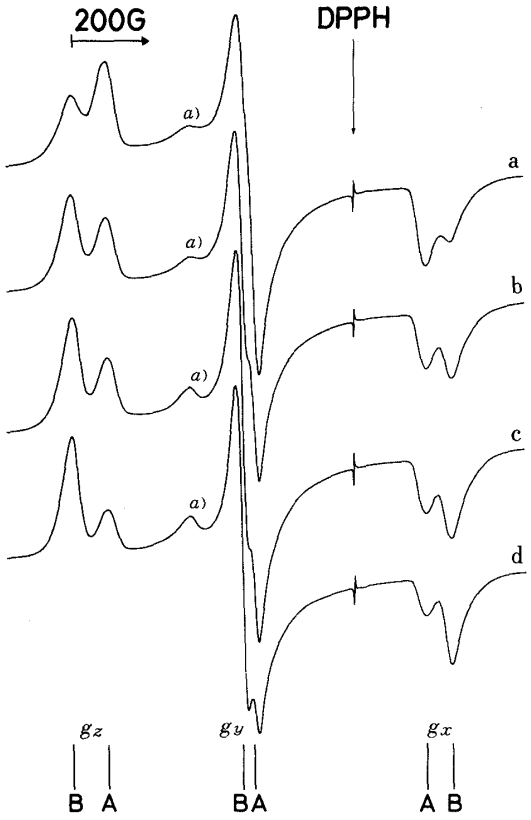

Fig. 3. Effect of MeOH Concentration on the EPR Spectra of Fe(TPP) (OMe) (NMeIm) in Me_2SO–MeOH at 20 K

Conditions: $[Fe(TPP)(OMe)]_0 = 0.70$ mM; $[NMeIm]_0/[Fe(TPP)(OMe)]_0 = 180$; MeOH concentration = 2.5% (v/v) (a), 5.0% (v/v) (b), 10% (v/v) (c), and 25% (v/v) (d). Peak assignments of g_x, g_y, and g_z absorptions for species A and B of Fe(TPP) (OMe) (NMeIm) are indicated at the bottom. Absorption peaks *a*) are due to Fe(TPP) $(NMeIm)_2^+$.

the concentration of solvent MeOH, free NMeIm, or added N-base such as lut, coll, or phen. In contrast, the g values of the two species were little affected by the concentration of each constituent in the system or by the sample temperature (Table I).

(a) Effect of MeOH Concentration——As pointed out in the preceding section, the presence of MeOH in the solvent systems is responsible for the two distinct low-spin species A and B. This, in turn, is suggestive of a mechanism of H-bonding interaction, since MeOH acts as an H-bond donor toward the coordinated MeO^- in Fe(TPP) (OMe) (NMeIm). To confirm such H-bonding interaction, EPR spectra of Fe(TPP) (OMe) (NMeIm) were observed in the mixed solvent Me_2SO–MeOH with various MeOH concentrations. Some typical spectra obtained at 20 K are shown in Fig. 3. It can be seen that species A exists in preference to B in the solvent at low MeOH concentration (*ca.* 2% (v/v)). An increase in MeOH concentration results in a gradual conversion from species A to B; the two species show nearly equal spectral intensities at the MeOH concentration of *ca.* 4.5% (v/v), and species B predominates at higher MeOH concentrations (>10% (v/v)). These observations are compatible with H-bond formation between the coordinated MeO^- and the solvent MeOH. The H-bond formation proceeds in one step, by EPR criteria, and species A and B are regarded as being in the initial and final H-bonded states, respectively, under the conditions studied.

(b) Effect of NMeIm Concentration——The interconversion of species A and B is also effected by change in NMeIm concentration. A typical spectral change is illustrated in Fig. 1. The spectrum of species A increases in intensity with a concomitant decrease in that of species B when the NMeIm concentration is successively increased. Clearly, excess free NMeIm causes species B to convert into A. This effect of NMeIm concentration offers a sharp contrast to that of MeOH concentration, but parallels that of lut concentration given below.

(c) Effect of lut Concentration——The ligands lut, coll, and phen are known to be particularly useful as H-bond acceptors because they are too sterically hindered to replace axially coordinated ligands in heme complexes.[13] In the present study, these N-bases have

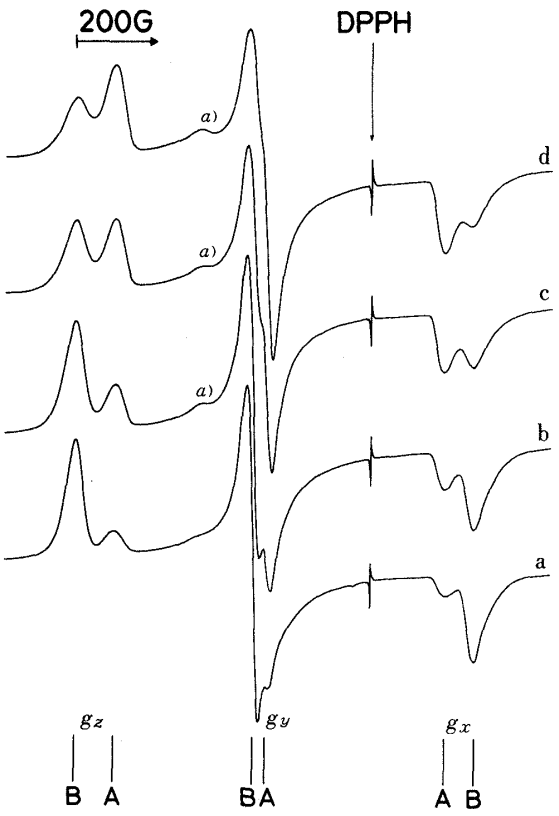

Fig. 4. Effect of lut Concentration on the EPR Spectra of Fe(TPP) (OMe) (NMeIm) in Me_2-SO–MeOH (90 : 10, v/v) at 20 K

Conditions: $[Fe(TPP)(OMe)]_0 = 0.30$ mM; $[NMeIm]_0/[Fe(TPP)(OMe)]_0 = 10$; $[lut]_0 = 0$ mM (a), 200 mM (b), 500 mM (c), and 700 mM (d). Peak assignments of g_x, g_y, and g_z absorptions for species A and B of Fe(TPP) (OMe) (NMeIm) are indicated at the bottom. Absorption peaks *a*) are due to Fe(TPP) $(NMeIm)_2^+$.

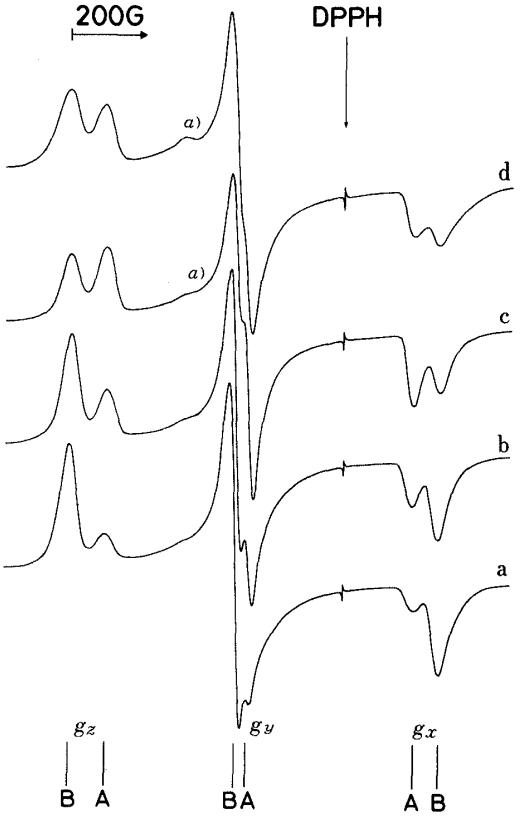

Fig. 5. Effect of Added coll and phen on the EPR Spectra of Fe(TPP) (OMe) (NMeIm) in Me_2SO–MeOH (90 : 10, v/v) at 20 K

Conditions: $[Fe(TPP)(OMe)]_0 = 0.70$ mM; $[NMeIm]_0/[Fe(TPP)(OMe)]_0 = 4.0$; added base and concentration, none (a), $[coll]_0 = 200$ mM (b), $[coll]_0 = 500$ mM (c), and $[phen]_0 = 200$ mM (d). Peak assignments of g_x, g_y, and g_z absorptions for species A and B of Fe(TPP) (OMe) (NMeIm) are indicated at the bottom. Absorption peaks *a*) are due to Fe(TPP) $(NMeIm)_2^+$.

been used to verify that the interconversion of species A and B is indeed due to the H-bonding interaction between the coordinated MeO^- and the solvent MeOH. It is expected that lut, coll, and phen would H-bond to MeOH when added to Me_2SO–MeOH, thereby decreasing the concentration of MeOH available to the coordinated MeO^- and in effect causing species B to convert into A. Figure 4 shows the spectral changes observed when various amounts of lut were added to Fe(TPP) (OMe) (NMeIm) in Me_2SO–MeOH. In accord with the above expectation, it was found that Fe(TPP) (OMe) (NMeIm) varies in its H-bonded state from species B to A with increasing lut concentration. Probably, lut competes with the coordinated MeO^- for H-bond formation to the solvent MeOH. Similar results were obtained with coll and phen (Fig. 5), confirming that the two low-spin species A and B differ in their H-bonded states.

(d) Hydrogen-Bond Formation Equilibria——Since no low-spin species other than A and B was detected for Fe(TPP) (OMe) (NMeIm) under the conditions studied, A and B are regarded as the initial and final H-bonded species, respectively. It is assumed, for simplicity, that the H-bonded states for A and B are as depicted in Chart 1. This model closely resembles the one proposed previously for the H-bonded species of Fe(TPP) $(OMe)_2^-$,[9] and leads us to explain the interconversion of species A and B in a similar way.

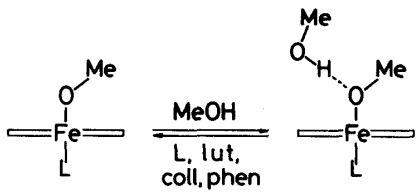

species A species B

L = NMeIm, py

Chart 1

In brief, the H-bond formation equilibria involved are written as:

$$MeOH + Me_2SO = MeOH \ldots OSMe_2 \quad (3)$$

$$MeOH + NMeIm = MeOH \ldots (NMeIm) \quad (4)$$

$$MeOH + lut = MeOH \ldots (lut) \quad (5)$$

$$MeOH + MeO\text{–}Fe = MeOH \ldots (MeO\text{–}Fe) \quad (6)$$

where MeO–Fe represents the coordinated MeO^- in Fe(TPP) (OMe) (NMeIm) and reaction 6 corresponds to the equilibrium between species A and B. MeO–Fe competes with Me_2SO, NMeIm, and lut for formation of an H bond to MeOH. It follows that the interconversion of species A and B is regulated by the concentration of free MeOH which varies *via* reactions 3—5 depending upon the concentrations of MeOH, NMeIm, and lut added to the system. All the observations given in (a), (b), and (c) can be reasonably explained by considering these H-bond formation equilibria. The effect of added coll and phen is explicable by introducing the H-bond formation equilibria (7) and (8) instead of (5):

$$MeOH + coll = MeOH \ldots (coll) \quad (7)$$

$$MeOH + phen = MeOH \ldots (phen) \quad (8)$$

The MeOH concentration at 50% H-bond formation in reaction 6 is a measure of the stability of the H bond in species B, since the reciprocal of the concentration is approximated to the formation or the stability constant. This MeOH concentration was found to increase with an increase in N-base concentration. At $[NMeIm]_0 = 125$ mM, the MeOH concentration at 50% H-bond formation was found to be *ca.* 4.5% (v/v) for Fe(TPP) (OMe) (NMeIm) in Me_2SO–MeOH. This value is much larger than the corresponding one (1—2% (v/v)) obtained for the H-bonded species of Fe(TPP) $(OMe)_2^-$ in Me_2SO–MeOH under similar conditions,[9] indicating that H-bonding interaction between the coordinated MeO^- and solvent MeOH is considerably weaker in Fe(TPP) (OMe) (NMeIm) than in Fe(TPP) $(OMe)_2^-$. This difference is attributed to a *trans* effect. *Trans* axial ligands with anionic rather than neutral character are more effective in stabilizing the H-bonding MeOH ... (MeO–Fe).

Interconversion of Hydrogen-Bonded States. Other Systems

The interconversion of H-bonded states A and B was also observed in the systems Fe-(TPP) (OMe) (NMeIm) in CH_2Cl_2–MeOH and toluene–MeOH and in the systems Fe(TPP) (OMe) (py) in Me_2SO–MeOH, CH_2Cl_2–MeOH, and toluene–MeOH. The interconversion behavior in these systems was functionally the same as that described in the preceding section for Fe (TPP)(OMe) (NMeIm) in Me_2SO–MeOH. Namely, an increase in MeOH concentration always caused species A to convert into B, while the reverse transformation B to A took place upon addition of H-bond acceptors such as NMeIm, py, lut, coll, and phen. However, no definite correlation has so far been found among the stability of the H bonding

MeOH...(MeO–Fe), the *trans* axial ligands (NMeIm and py), and the solvent systems (Me_2SO–, CH_2Cl_2–, and toluene–MeOH).

It should be noted here that the g values for species A of Fe(TPP) (OMe) (NMeIm) and Fe(TPP) (OMe) (py) are found to vary by some slight but significant amount depending upon the solvent systems Me_2SO–MeOH, CH_2Cl_2–MeOH, and toluene–MeOH, while those for species B remain almost constant among the three solvent systems (Table I). It is very likely that there is a weak interaction in species A between the coordinated MeO^- and the solvent molecule such as Me_2SO, CH_2Cl_2, or toluene. The g anisotropies for Fe(TPP) (OMe) (NMeIm) and Fe(TPP) (OMe) (py) in the three solvent systems increase remarkably on going from species A to B, *i.e.*, upon formation of the H bond MeOH...(MeO–Fe). The g anisotropies for species A, which increase slightly in the order of increasing solvent acceptor number,[14] indicate that the interaction involved in species A is a weak H bonding of the type (solvent)...(MeO–Fe). In Chart 1, such a weak H-bonding interaction in species A is omitted for brevity. In contrast, the fact that the g anisotropies for species B are not affected by the solvent systems supports the view that the coordinated MeO^- in species B is strongly H-bonded to the solvent MeOH, as depicted in Chart 1.

Hydrogen Bonding and Crystal Field Splittings

To demonstrate the electronic alterations at the central metal ion caused by the H-bonding interaction in the axial ligand, we have analyzed the g values observed for the H-bonded species A and B with the assumption of a pure t_2^5 electron configuration as described previously.[16] The tetragonal and rhombic splittings in the t_2 orbitals (*i.e.*, d_{yz}, d_{zx}, and d_{xy}), δ and μ,[17] respectively, the crystal field rhombicity R defined as the quantity μ/δ, and the orbital reduction factor k are determined from the three observed values (g_x, g_y, g_z). Such crystal field

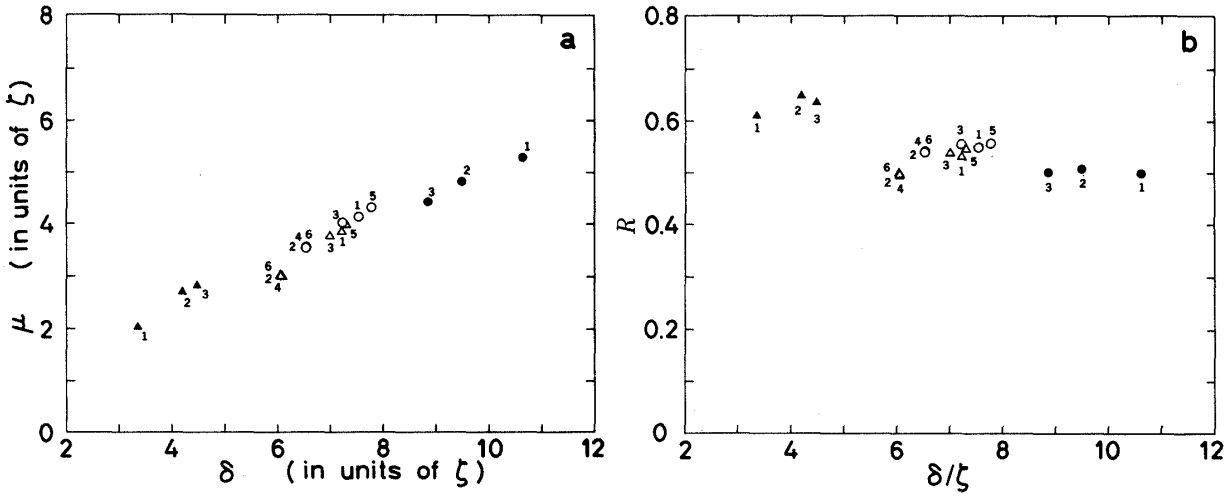

Fig. 6. Crystal Field Diagrams for Hydrogen-Bonded Low-Spin Fe(III) Heme Complexes. (a) Rhombic Splitting *versus* Tetragonal Splitting (μ *vs.* δ) and (b) Crystal Field Rhombicity *versus* Tetragonality (R *vs.* δ/ζ)

○ for Fe(TPP) (OMe) (NMeIm): 1, species A/Me_2SO–MeOH; 2, species B/Me_2SO–MeOH; 3, species A/CH_2Cl_2–MeOH; 4, species B/CH_2Cl_2–MeOH; 5, species A/toluene–MeOH; 6, species B/toluene–MeOH.

△ for Fe(TPP) (OMe) (py): 1, species A/Me_2SO–MeOH; 2, species B/Me_2SO–MeOH; 3, species A/CH_2Cl_2–MeOH; 4, species B/CH_2Cl_2–MeOH; 5, species A/toluene–MeOH; 6, species B/toluene–MeOH (crystal field values at 20 K are plotted).

● for Fe(TPP) $(OMe)_2^-$/Me_2SO–MeOH: 1, species I; 2, species II; 3, species III. For details, see reference 9.

▲ for H-bonded species of bis-imidazole complex in CH_2Cl_2: 1, axial ligands with no strong H-bonding interaction ($Fe(TPP)(ImH)_2^+$); 2, one imidazole ligand strongly H-bonded or deprotonated (Fe(TPP)(Im)(ImH)); 3, two imidazole ligands strongly H-bonded or deprotonated ($Fe(TPP)(Im)_2^-$). For details, see reference 7.

parameters are summarized in Table I and Fig. 6, where the values are compared with those obtained for the H-bonded species of Fe(TPP) $(OMe)_2^-$ [9] and Fe(TPP) $(ImH)_2^+$.[7]

(a) Orbital Reduction Factor——As may be seen from Table I, the orbital reduction factor k remains almost constant among the H-bonded species of Fe(TPP) (OMe) (NMeIm) and Fe(TPP) (OMe) (py) in the three solvent systems. The k values fall within the range from 1.0 to 1.1, indicating that the H-bonded species A and B belong to the normal class of low-spin Fe(III) heme complexes. The same is true of the H-bonded species of Fe(TPP) $(OMe)_2$ and Fe(TPP) $(ImH)_2^+$.

The relation $k > 1$ implies an increase in the orbital angular momentum of the ground $^2T_2$ state. Such an apparent anomaly in k can be removed easily, if we take into consideration the electrostatic and spin-orbit admixtures of excited t_2^4e states into the ground $t_2^5\ ^2T_2$ state.[16,18] In the present work, however, the crystal field parameters δ, μ, R, and k were not corrected for the effect of admixture of excited states, since a method of g value analysis including the excited states results in much complication and ambiguity in numerical procedures. The simple analysis based on the pure t_2^5 electron configuration is sufficient for our present purpose.

(b) Tetragonal and Rhombic Splittings——In species A, the tetragonal and rhombic splittings (δ and μ) are both affected appreciably by change in solvent system, while, in species B, they are not (Fig. 6a). This is in accord with the H-bonded structures of species A and B discussed in the preceding section. The increasing order of the δ and μ values for species A in the three solvent systems follows the decreasing order of solvent acceptor number ($CH_2Cl_2 > Me_2SO >$ toluene),[14] showing an important role of weak H-bonding interaction between the coordinated MeO^- and surrounding solvent molecules. In species B, the H bonding MeOH...(MeO–Fe) is too strong to be replaced by the solvent molecules and the δ and μ values remain unaffected by the solvent systems.

Most important, the δ and μ values for Fe(TPP) (OMe) (NMeIm) and Fe(TPP) (OMe) (py) decrease markedly on going from the H-bonded state A to B, indicating that the strong H-bonding interaction between the coordinated MeO^- and the solvent MeOH leads to a decreased crystal field at the iron. Such decreases in the values of δ and μ with increasing H-bonding interaction parallel the trend found in Fe(TPP) $(OMe)_2^-$ [9] but are opposite to that in Fe(TPP) $(ImH)_2^+$.[7,8] These opposite trends in crystal field alterations are quite reasonable in that the coordinated MeO^- ligand acts as a proton acceptor toward the solvent MeOH, while the coordinated ImH ligand acts as a proton donor toward external H-bonders.

The parameter δ is related to the strength of the tetragonal field sensed by the iron t_2 orbitals, which in turn reflects, in the framework of the molecular orbital (MO) method, the strength of π bonding interaction between the iron and axial-ligand orbitals. Thus, the stronger the electron donor properties of the axial ligand, the larger will be the value of δ and the electron density to be expected at the iron.[19,20] The observed changes in δ are, therefore, taken to indicate that the H-bonding interaction in Fe(TPP) (OMe) (NMeIm), Fe(TPP) (OMe) (py), and Fe(TPP) $(OMe)_2^-$ reduces the π donor strength of the axial MeO^- ligand, thereby decreasing the crystal field and the electron density at the iron. The reverse is true of the H-bonding interaction in Fe(TPP) $(ImH)_2^+$.

The above interpretation can be rationalized qualitatively by *ab initio* MO calculations for metal-free H-bonded systems of the type X–H...Y.[21] The calculated results worthy of remark are: (1) all the MO's on the proton donor (X) increase in energy upon H-bond formation, while those on the proton acceptor (Y) decrease, and (2) the H-bond formation causes electron redistribution: H loses electrons, X and Y gain electrons (more electrons are gained by X), electrons are transferred from Y to X, and atoms immediately attached to X and Y gain and lose electrons, respectively. If such MO energy shifts and electron redistributions are valid for the H-bonded systems M–L...H–X and M–L–H...Y (where

M–L and M–L–H refer to the metal-bound ligands with proton acceptor and donor properties, respectively), the following are the electronic alterations expected to be caused by the H-bonding interaction M–L...H–X: (1) the MO's on L with σ- and π-donor characters toward the metal ion M decrease in energy, and (2) the electron density at M decreases, resulting in a decreasing metal-ligand interaction. The reverse is the case with the H-bonded system M–L–H...Y. These predictions are indeed consistent with the information obtained from the crystal field parameters, which, in turn, supports the view that the tetragonal splitting δ is a measure of electron density at the iron. However, it should be noted that the electron density is affected rather strongly by change in metal-ligand σ interaction, while the value δ is solely determined by metal-ligand π interaction.

(c) Crystal Field Rhombicity——In contrast to the significant variations in δ and μ with H-bonding interactions, the R values are found to be almost independent of the H-bonded states, as may be seen from Fig. 6b. According to the crystal field calculation[22] based on the point charge model, the crystal field rhombicity R defined as the quantity μ/δ is a purely geometric factor only when the fourth-order components in the tetragonal and rhombic crystal field potentials are negligibly small compared to the second-order ones or *vice versa*. On the other hand, the value R is related to the geometrical arrangement of axial ligands. In particular, for complexes where the axial ligands are chemically equivalent and approximately parallel or where the interactions with one of the axial ligands dominate, R is a good measure of the intrinsic asymmetry of the axial ligand.[23]

In the present complexes, the MeO^- ligand seems to play a dominant role in determining the crystal field splittings so that the R values of Fe(TPP) (OMe) (NMeIm) are almost the same as those of Fe(TPP) (OMe) (py). The analyses of EPR data for Fe(p) (OR) L,[9,10,12,24,25] where p = TPP, OEP, PPIXDME, $RO^- = MeO^-$, EtO^-, PhO^-, and L = MeO^-, EtO^-, ImH, NMeIm, py, pip, *etc.*, have shown that the intrinsic asymmetry of RO^- ligands is in the range of $R = 0.45$—0.60, which is much smaller than the intrinsic asymmetry $R = 0.9$—1.2 of axial thiolate ligands.[12,23] The values $R = 0.49$—0.50 obtained previously for Fe(TPP) $(OMe)_2^-$ [9] strongly suggest that the two axial MeO^- ligands are in approximately parallel orientations. The values $R = 0.49$—0.56 obtained in the present work for the H-bonded species A and B of Fe(TPP) (OMe) (NMeIm) and Fe(TPP) (OMe) (py), which are well within the intrinsic asymmetry range of RO^- ligands, are taken to indicate that the interactions with the MeO^- ligand dominate and that species A and B have similar geometrical arrangements of axial ligands. In the light of the results on the H-bonded states of Fe(TPP) $(OMe)_2^-$, we are led to the view that the H-bond formation does not alter the geometry of the nearest coordination sphere of Fe(TPP) (OMe) (NMeIm) and Fe(TPP) (OMe) (py). The same can be said of the geometrical arrangements of axial ligands in the H-bonded species of Fe(TPP) $(ImH)_2^+$, since the R values are in the narrow range from 0.61 to 0.65.[7,8]

Conclusions

It has been demonstrated that the H-bonding interactions in the axial ligands of iron porphyrin complexes modulate the electronic properties at the central metal ion. In general, the H-bond formation involving the axial ligand acting as a proton acceptor leads to a decreased crystal field and electron density at the iron, and the reverse is true of the axial ligand acting as a proton donor. The H-bonding interactions do not alter the geometrical arrangements of the nearest coordination sphere of iron porphyrin complexes.

References and Notes

1) M. A. Stanford, J. C. Swartz, T. E. Phillips, and B. M. Hoffman, *J. Am. Chem. Soc.*, **102**, 4492 (1980).

2) R. Quinn, J. Mercer-Smith, J. N. Burstyn, and J. S. Valentine, *J. Am. Chem. Soc.*, **106**, 4136 (1984).
3) J. G. Jones, G. A. Tondreau, J. O. Edwards, and D. A. Sweigart, *Inorg. Chem.*, **24**, 296 (1985); P. O'Brien and D. A. Sweigart, *ibid.*, **24**, 1405 (1985) and references therein.
4) Abbreviations: TPP, tetraphenylporphine dianion; PPIX, protoporphyrin IX dianion; PPIXDME, protoporphyrin IX dimethyl ester dianion; OEP, octaethylporphyrin dianion; ImH, imidazole; NMeIm, *N*-methylimidazole; py, pyridine; phen, 1,10-phenanthroline; lut, 2,6-lutidine; coll, 2,4,6-collidine; pip, piperidine; EPR, electron paramagnetic resonance; DPPH, diphenylpicrylhydrazyl.
5) J. Peisach, W. E. Blumberg, and A. Adler, *Ann. N. Y. Acad. Sci.*, **206**, 310 (1973).
6) T. Yoshimura and T. Ozaki, *Arch. Biochem. Biophys.*, **230**, 466 (1984).
7) R. Quinn, M. Nappa, and J. S. Valentine, *J. Am. Chem. Soc.*, **104**, 2588 (1982).
8) F. A. Walker, D. Reis, and V. L. Balke, *J. Am. Chem. Soc.*, **106**, 6888 (1984).
9) T. Otsuka, T. Ohya, and M. Sato, *Inorg. Chem.*, **24**, 776 (1985).
10) T. Otsuka, T. Ohya, and M. Sato, *Inorg. Chem.*, **23**, 1777 (1984).
11) A. D. Adler, F. R. Longo, J. D. Finarelli, J. Goldmacher, J. Assour, and L. Korsakoff, *J. Org. Chem.*, **32**, 476 (1967); G. H. Barnett, M. F. Hudson, and K. M. Smith, *Tetrahedron Lett.*, **1973**, 2887.
12) S. C. Tang, S. Koch, G. C. Papaefthymiou, S. Foner, R. B. Frankel, J. A. Ibers, and R. H. Holm, *J. Am. Chem. Soc.*, **98**, 2414 (1976).
13) A. L. Balch, J. J. Watkins, and D. J. Doonan, *Inorg. Chem.*, **18**, 1228 (1979).
14) Solvent acceptor number: toluene, ~8 (estimated from the value for benzene); Me_2SO, 19.3; CH_2Cl_2, 20.4.[15]
15) V. Gutmann, "The Donor–Acceptor Approach to Molecular Interaction," Plenum Press, New York, 1978, p. 17.
16) M. Sato, T. Ohya, and I. Morishima, *Mol. Phys.*, **42**, 475 (1981).
17) We follow Weissbluth in using the symbols δ and μ to represent the tetragonal and rhombic splittings, respectively (M. Weissbluth, *Struct. Bonding* (Berlin), **2**, 1 (1967)).
18) J. S. Griffith, *Mol. Phys.*, **21**, 135 (1971).
19) This relation is based on the magnetic axis system in which the tetragonal field component is referred to the heme normal. Note that Blumberg and Peisach used a different axis system in their earlier publications.[20] They found the reverse relation, that the value δ decreases with increasing electron density at the iron.
20) W. E. Blumberg and J. Peisach, "Probes of Structure and Function of Macromolecules and Membranes," Vol. 2, ed. by B. Chance, T. Yonetani, and A. S. Mildvan, Academic Press, New York, 1971, p. 215; W. E. Blumberg and J. Peisach, *Adv. Chem. Ser.*, **100**, 271 (1971).
21) P. A. Kollman and L. C. Allen, *Chem. Rev.*, **72**, 283 (1972); S. Yamabe and K. Morokuma, *J. Am. Chem. Soc.*, **97**, 4458 (1975); H. Umeyama and K. Morokuma, *ibid.*, **99**, 1316 (1977).
22) See for example: R. R. Sharma, T. P. Das, and R. Orbach, *Phys. Rev.*, **149**, 257 (1966); M. Sato, A. S. Rispin, and H. Kon, *Chem. Phys.*, **18**, 211 (1976).
23) M. P. Byrn, B. A. Katz, N. L. Keder, K. R. Levan, C. J. Magurany, K. M. Miller, J. W. Pritt, and C. E. Strouse, *J. Am. Chem. Soc.*, **105**, 4916 (1983).
24) E. W. Ainscough, A. W. Addison, D. Dolphin, and B. R. James, *J. Am. Chem. Soc.*, **100**, 7585 (1978).
25) T. Otsuka and M. Sato, unpublished.